

1 The process control of the triple-column pressure-swing extractive  
2 distillation with partial heat integration

3 Tao Shi<sup>1,2</sup>, Wei Chun<sup>3</sup>, Ao Yang<sup>1,2</sup>, Saimeng Jin<sup>1,2</sup>, Weifeng Shen<sup>1,2,\*</sup>, Jingzheng Ren<sup>4</sup>, Jinglian Gu<sup>5</sup>

4 <sup>1</sup>School of Chemistry and Chemical Engineering, Chongqing University, Chongqing 400044, P. R.  
5 China

6 <sup>2</sup>National-municipal Joint Engineering laboratory for Chemical Process Intensification and Reaction,  
7 Chongqing University, Chongqing 400044, P. R. China

8 <sup>3</sup>School of Economics and Business Administration, Chongqing University, Chongqing 400044, P.R.  
9 China

10 <sup>4</sup>Department of Industrial and Systems Engineering, The Hong Kong Polytechnic University, Hong  
11 Kong SAR, P. R. China

12 <sup>5</sup>Fujian Universities Engineering Research Center of Reactive Distillation Technology, College of  
13 Chemical Engineering, Fuzhou University, Fuzhou 350116, Fujian China

14 **Corresponding Author:** \*(W.S) E-mail: [shenweifeng@cqu.edu.cn](mailto:shenweifeng@cqu.edu.cn)

15 **Abstract**

16 Recently, increasing researches have focused on the intensified heat-integrated triple-column  
17 pressure-swing extractive distillation (HITPED) owing to its superiority in economic and  
18 environmental benefits than the conventional extractive distillation. However, the dynamic  
19 controllability investigation for HITPED was lacking, resulting in the difficulties for industrial  
20 application. Therefore, separating the ternary azeotropic mixture tetrahydrofuran  
21 (THF)-methanol-water by HITPED is taken as an example to fully investigate the dynamic  
22 controllability. On the basis of the open-loop analysis a basic control structure CS1 is firstly  
23 proposed. To deal with the 20% disturbance in feed composition more effectively, the CS2 with a  
24 low selector and composition controllers is then developed. Nevertheless, composition controllers  
25 are less applied in chemical industry than temperature controllers owing to the long delay and high  
26 cost. As such, two different control structures (CS3 and CS4) without any composition controllers  
27 are then put forward. Integral absolute error (IAE) is applied to compare the dynamic performance.  
28 Under the 20% disturbances of the feed flowrate and composition, the robust control strategy CS4  
29 with temperature controllers and a high selector exhibits the gratifying dynamic performance. The

1 application of the selector further enlarges the dynamic researches in the distillation process.

2 **Keywords:** Pressure-swing extractive distillation, Partial heat-integration process, Dynamic control,  
3 Separation, Azeotropic mixture

## 4 1. Introduction

5 The distillation, as an commonly technique for the separation of the solvent mixture, is widely  
6 applied in the chemical industry [1]. However, inevitable existing azeotropic mixtures in chemical  
7 processes are impossible to be separated by the conventional distillation. Therefore, special  
8 distillation schemes such as pressure-swing distillation (PSD) [2-4], azeotropic distillation (AD) [5, 6]  
9 and extractive distillation (ED) [7-9] are proposed. Of note is that the energy consumption in these  
10 schemes is high. To achieve the energy-saving performance, some methods of the process  
11 intensification are applied in the special distillations.

12 PSD is one of the viable strategies for separating the pressure-sensitive azeotropic mixtures, in  
13 which high-pressure and low-pressure distillation columns are combined to cross the azeotropic point.  
14 And the heat integration was easily obtained through the pressure changes between the distillation  
15 columns [10]. For instance, Zhu et al. [11] proposed a heat-integrated PSD scheme for separating the  
16 minimum boiling mixture toluene-ethanol and they illustrated the proposed configuration is more  
17 economical than the conventional design without heat integration. Zhang et al. [12] explored the  
18 design and controllability of partial and fully heat-integration PSD for the separation of ethyl acetate  
19 and ethanol, and the scheme with fully heat integration is found to be more superior in lower energy  
20 consumption and CO<sub>2</sub> emission. For the design and control of the separating binary azeotropic  
21 mixture dichloromethane/methanol, the heat-integrated PSD, as one of feasible schemes, was  
22 proposed by Iqbal et al. [13]. Up to now, the separation of the ternary azeotropic mixtures such as  
23 acetonitrile/methanol/benzene [14], THF/ethanol/water [15], methanol/methyl acetate/acetaldehyde  
24 [16] and diisopropylether/isopropanol/water [17] through heat-integrated PSD greatly enlarged the  
25 research filed and the triple-column PSD with heat-integration has shown its advancement in smaller  
26 energy cost [18]. However, very few effective control structures have been reported for the  
27 complicated triple-column PSD processes with heat integration, especially by temperature controllers  
28 when the 20% disturbances are introduced to the feed flowrate and the composition.

29 For the energy-saving investigations of the ED process, Tututi-Avila et al. [19] proposed a novel

1 side-stream ED process and the heat integration between distillation columns can be considered for  
2 further energy savings. Yang et al. [20] designed an optimal extractive dividing-wall column with a  
3 preheater to achieve the separation of methanol/toluene/water and the results have proved that the  
4 intensified scheme can reduced the total annual cost by 15.14% than the traditional ED process.  
5 Besides, the heat-pump configuration can be combined with the ED process to full utilize the latent  
6 heat of steam [21]. Of note is that the intensified ED process through varying pressure has attracted  
7 the attention for dramatically improving the relative volatility. Thereby, the heat integration between  
8 distillation columns can be obtained to save more energy than the conventional ED scheme.  
9 Previously, You et al. [22] proposed a novel pressures-swing ED strategy for the separation of the  
10 pressure-sensitive azeotropic mixture acetone/methanol and the proposed scheme attained 33.9% and  
11 30.1% reductions in the energy consumption and the total annual cost, which implies the significant  
12 impact of an optimum pressure to the determination of the ED design. Yang et al. applied the  
13 pressure-swing ED for separating the binary azeotropic mixture ethanol/dimethyl carbonate [23] and  
14 ternary azeotropic mixture ethyl acetate/ethanol/water [24], both of the results have shown its  
15 superiority in decreasing the energy consumption due to the improved relative volatility. To separate  
16 pressure-insensitive minimum boiling azeotrope methanol/toluene, the heat-integrated ED process  
17 with pressure changes was also utilized [25]. Although the proposed heat-integrated pressure-swing  
18 ED process has effectively reduced the energy consumption, it makes the process control become  
19 more difficult than the conventional process because the additional entrainer is added. The amount of  
20 the entrainer influence the product quality in the ED process, another entrainer and heat integration  
21 in pressure-swing ED process greatly increase the complexity of the control scheme. So far, there has  
22 been no effective published work in investigating the controllability of the PSD-ED process with  
23 heat integration. Presenting a robust control scheme for the intensified pressure-swing ED is  
24 significant.

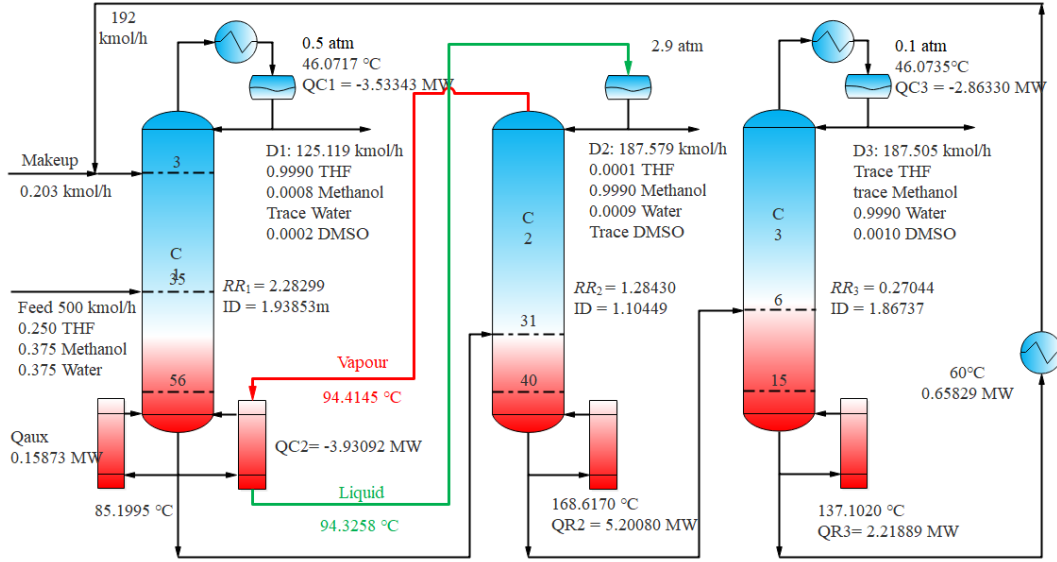
25 In terms of the dynamic controllability research for ED process, there are some common  
26 experiences from the previous works. For example, the bottom level of the last column is controlled  
27 by the make-up entrainer stream to avoid “snowball” effect, which was found by Luyben [26].  
28 Besides, the ratio of recycled flowrate of the entrainer and the feed flowrate ( $S/F$ ) was generally  
29 fixed in the dynamic control structures [24, 27]. However, in the control study of the heat-integrated  
30 ED, the nonlinear relationship between the entrainer and feed flowrate demonstrated that nonlinear

1 function should be proposed to improve the dynamic responds [28-30]. And it can be concluded from  
2 the research by Wang et al. [31] that the reflux ratio and reboiler duty of the ED column can be  
3 simultaneously adjusted to control the dual-temperature of specified stages. The dual-temperature  
4 control structure can provide a guideline for the dynamic research of the triple-column extractive  
5 distillation. Comparatively, the dynamic investigation of the PSD with heat-integration is much  
6 difficult due to the “free” pressure of a column in the dynamic design [32, 33]. Generally, a  
7 composition controller can improve the dynamic performances of the triple-column PSD especially  
8 under the 20% feed composition disturbance [18]. However, using composition controllers represents  
9 the long delay and great cost in the practical chemical industry [34]. To avoid this issue, Li et al. [35]  
10 explored the robust control strategies with the pressure-compensated temperature scheme for partial  
11 heat-integration PSD in one separation sequence.

12 From the review of the above studies, very few dynamic controllability studies can be found for  
13 an energy-saving scheme combining the heat-integration pressure-swing technique and the ED, let  
14 alone the triple-column distillation process. The novelty of the research is that we proposed a robust  
15 temperature control structure with selectors for the complicated heat intensified pressure-swing ED  
16 process. It is noteworthy that the proposed control structures can deal with the 20% disturbances in  
17 both feed flowrate and composition. The process control of the heat-integrated triple-column  
18 pressure-swing extractive distillation process (HITPED) is fully investigated based on the  
19 reproduced process by Gu et al [36]. For the separation of the ternary mixtures tetrahydrofuran  
20 (THF)/methanol/water, the partial HITPED process has been proved to be the most energy-saving in  
21 their work. However, whether the HITPED can be practically controlled under the different feed  
22 disturbances is still a problem and it is exact the main target of this work. Initially, an open-loop  
23 analysis is carried out to determine the sensitivity plates. Then, the basic control structure CS1 of the  
24 complicated scheme for separating THF/methanol/water is obtained by manipulating the temperature  
25 of the sensitive plates. To evaluate the stability and robustness of the proposed control strategies, the  
26  $\pm 20\%$  feed flow rates and the compositions disturbances are introduced and the integral absolute  
27 error (IAE) is calculated. Following that, the key ratio of the entrainer flowrate to the feed flowrate  
28 (abbreviated as S/F) is modified in other control structures CS2 and CS4. Wherein, a control  
29 structure CS2 is also featured by the composition-(S/F) cascade with a low selector. To develop an  
30 effective temperature control with lower delay and practical operation, the CS3 with single

1 temperature manipulating the reflux ratio and reboiler duty is presented. Based on the dynamic  
 2 response in CS3, we finally propose an improved control structure CS4 with temperature-(S/F)  
 3 cascade and a high selector.

4 **2. Steady-state process**



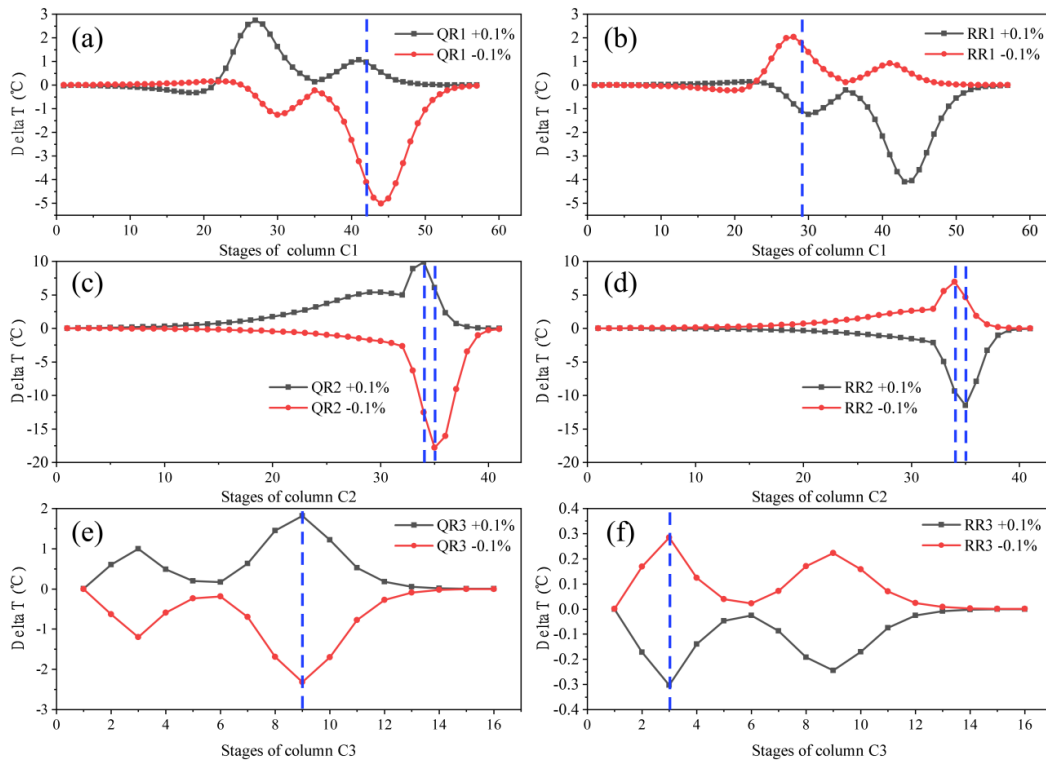
5  
6 **Fig.1** The partial HITPED for separating THF-methanol-water with DMSO entrainer

7 The steady-state process of this research is carried out in Aspen Plus. Because of the large  
 8 influence of thermodynamic proprieties on the separation process, the selection of a proper  
 9 thermodynamic model is important [37, 38]. On the basis of the existing separation process [36]  
 10 for the quaternary system with THF-methanol-water-dimethyl sulfoxide (DMSO), the nonrandom two  
 11 liquid (NRTL) property model is used to describe the non-ideality of the vapor-liquid equilibrium  
 12 (see **Table S1** in supporting information). **Fig.1** has demonstrated the reproduced process flowsheet  
 13 with detailed parameters. The feeding condition for separating THF-methanol-water is 500 kmol/h  
 14 fresh feed with the composition of 25 mol% THF, 37.5 mol% methanol and 37.5 mol% water at the  
 15 temperature of 30 °C in 1 atm. Pressures of three columns are 0.5, 2.9 and 0.1 atm respectively,  
 16 which permitting the distilled steam to transfer heat for heating the sump of the first column. Besides,  
 17 the pressure drops in three columns are 0.0068 atm. And “design specifications” are applied to  
 18 guarantee all the product purities with 99.9 mol% and the recovery fraction with 99.99 mol%.  
 19 Eventually, the reproduced HITPED process has slight differences in the reflux ratios as well as  
 20 distilled flowrates in comparison with the previous study [36]. However, this will not affect the  
 21 dynamic controllability investigation for the complicated process.

1 Before installing the dynamic design, some parameters are firstly set to carry out the pressure  
 2 checker. According to the study of Luyben [39], pumps and valves are expected to provide proper  
 3 pressure drops (*i.e.*, 3 atm) to deal with the feed disturbances without leading to the valve saturation.  
 4 And the “heuristic method” is used to determine the volumes of reflux drums and sumps which are  
 5 calculated with total 20 min holdup. The detailed dimensions of three column sumps and reflux  
 6 drums are summarized in **Table S2**. Then, the pressure-driven based dynamic process is achieved in  
 7 Aspen Plus Dynamics. To ensure the safety of the operation, several control variables such as feed  
 8 flowrates, liquid levels and pressure have to be maintained at or close to their set points. The product  
 9 purity is indicated by the specified tray temperature since the composition variation on each tray  
 10 depends on the corresponding tray temperature under specified pressure. Following which, 20% step  
 11 disturbances of feed flowrate and composition are introduced to test the process controllability.

## 12 3. Dynamic control

### 13 3.1 Determination of temperature control trays



14

15

**Fig.2** The open-loop sensitivity analysis for three columns

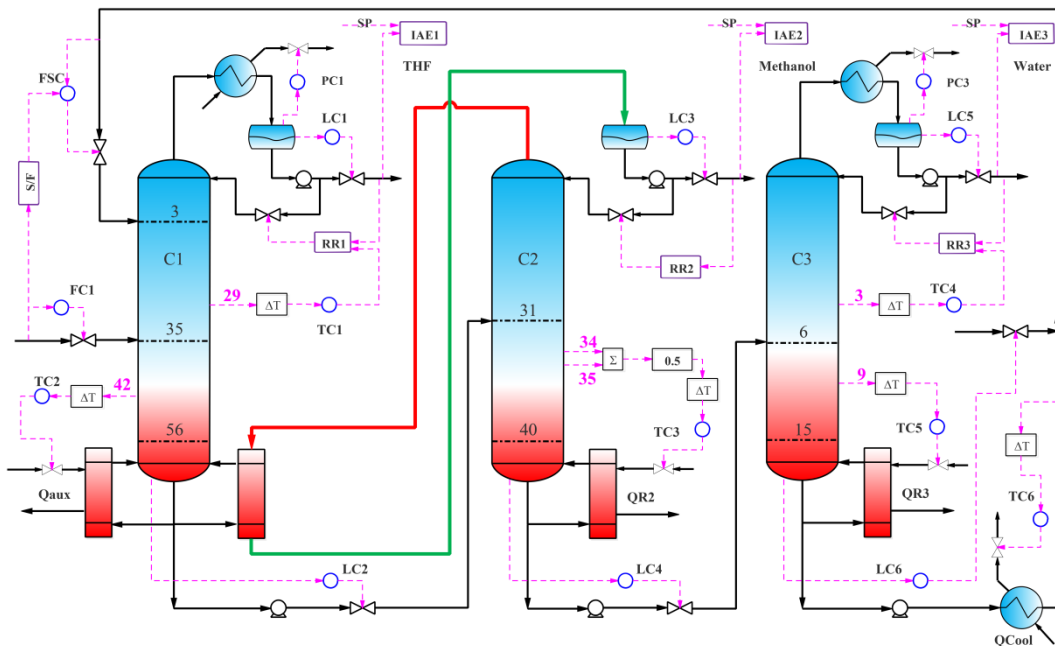
16

17

As the pressure of a column remains constant, the composition of the specified plate is determined by the temperature. The temperature-sensitive trays of three columns are selected *via* the

1 open-loop sensitivity analysis. The temperature gains in each tray can be obtained through varying  
 2 the reboiler duties (*i.e.*,  $QR1$ ,  $QR2$ ,  $QR3$ ) and the reflux ratios (*i.e.*,  $RR1$ ,  $RR2$ ,  $RR3$ ) by small ranges  
 3 ( $\pm 0.1\%$ ), as shown in **Fig.2**. It can be found from **Fig.2 (a)** that the temperature of 44th tray has the  
 4 largest gain under the changes of  $-0.1\%$   $QR1$  while the temperature of 41th tray exhibits a great  
 5 steady-state gain under the changes of  $+0.1\%$   $QR1$ . To make a compromise between the increased  
 6 and decreased changes and consider the heat integration, the 42th stage of the C1 column is selected  
 7 to adjust the auxiliary reboiler duty of C1 column (abbreviated as  $Q_{aux}$ ). Similarly shown in **Fig.2(b)**,  
 8 the 29th tray of the C1 column is the temperature control trays for adjusting the  $RR1$ . **Fig.2(c)** and **(d)**  
 9 demonstrates that both of 34th and 35th trays reflect the remarkable impact for the changes of  $QR2$   
 10 and  $RR2$ . In general, the reboiler duty can be manipulated timely without the hydraulics delay. As a  
 11 result, the average temperature of the 34th and 35th plates is proposed to control the  $QR2$  and the  
 12 fixed  $RR2$  is applied. As for the C3 column, the 3th and 9th stage are determined as the  
 13 temperature-sensitive stages to manipulate  $RR3$  and  $QR3$ , respectively. To virtually evaluate the  
 14 dynamic responses, the indicator IAE is calculated. The maximum transient deviation, oscillation  
 15 amplitude and stabilized offset are the main considerations for evaluating the distillation control  
 16 system, which directly affects the value of IAE [29].

### 17 3.3 The basic control structure CS1



18 **Fig.3** The basic control structure with dual-temperature of the HITPED process  
 19

1 In this work, the gain ( $K_c$ ) and the integral time ( $\tau_I$ ) of the flow controllers (*i.e.*, FC1 and FSC)  
 2 are 0.5 and 0.3 min, respectively. The  $K_c$  and  $\tau_I$  of pressure controllers (*i.e.* PC1 and PC3) are 20  
 3 and 12 min. All level controllers (*i.e.*, LC1, LC2, LC3, LC4, LC5 and LC6) are set with only  
 4 proportion control with  $K_c=2$  and  $\tau_I=9999$  min. The suitable  $K_c$  and  $\tau_I$  of other temperature  
 5 controllers (*e.g.*, TC1) are tuned by the Tyreus–Luyben method (see in **eq.(1)-(2)**) after  
 6 relay-feedback tests, and the dead time of the temperature controllers is given as 1 min [40].

$$7 \quad K_c = K_U / 3.2 \quad (1)$$

$$8 \quad \tau_I = 2.2 P_U \quad (2)$$

9 The basic control scheme (CS1) is illustrated in **Fig.3** according to results in **Section 3.1**. The  
 10 detailed control loops are listed as follows:

- 11 (1) Both of the fresh feed controller (FC1) and entrainer flowrate controller (FSC) are set as the  
 12 reverse action. The S/F value is fixed by a Multiply module in the exported dynamic file.
- 13 (2) The base levels of all the reflux drums are controlled by manipulating the distilled flowrate  
 14 with direct action, which are achieved by level controllers (LC1, LC3 and LC5).
- 15 (3) The sump levels in the C1 and C2 columns are controlled by operating the bottom flowrates  
 16 with direct action (see LC2 and LC4 controllers). However, the sump level in C3 column is  
 17 timely adjusted by LC6 controller with reverse action by manipulating the flowrate of the  
 18 make-up entrainer.
- 19 (4) For the control of C1 column, the temperature of 29th stage and 42th stage are used to adjust  
 20 the  $RR1$  and  $Q_{aux}$ , which are finished by the TC1 and TC2 controllers.
- 21 (5) For the control of C2 column, the TC3 controller with reverse action is applied to realize the  
 22 control of the average temperature of 34th and 35th stages. Meanwhile the  $RR2$  is fixed since  
 23 no other sensitivity stages can be used.
- 24 (6) For the control of C3 column, the TC4 controller with direct action timely modifies the  $RR2$   
 25 according to the signal of the temperature of 3th stage. And the TC5 controller with reverse  
 26 action modifies the  $QR3$  based on the temperature of the 9th tray.
- 27 (7) The temperature of the recycled entrainer is cooled by the TC6 controller with reverse action.  
 28 The partial heat integration in the dynamic investigation is achieved by the “flowsheet function”.



1 The **eq.(3)** is applied to calculate the condenser duty of the C2 column (abbreviated as  $QC2$ ). The  
 2 overall heat transfer coefficient  $K$  is assumed to  $0.00306 \text{ GJ}/(\text{h}\cdot\text{m}^2\cdot^\circ\text{C})$  according to Luyben et al.  
 3 [40], which can be applied to calculate the transfer area  $A_C$  of the heat exchanger (approximately  
 4  $506.734 \text{ m}^2$ ). According to the results in steady-state HITPED process, the auxiliary reboiler duty of  
 5 C1 column  $Q_{aux}$  is equal to  $0.15873 \text{ MW}$ . As shown in the **eq.(4)**, the total reboiler duty of C1  
 6 column  $QR1$  is the sum of  $Q_{aux}$  and absolute value  $QC2$ .

$$7 \quad QC2 = K \cdot A_C \cdot \Delta t \quad (3)$$

$$8 \quad QR1 = Q_{aux} + QC2 \quad (4)$$

9 And the whole “flowsheet function” in Aspen Plus Dynamics is given as follows,

10 Constraints

11 `Blocks(“C2”).Condenser(1).Q=-0.00306*506.734*(Blocks(“C2”).Stage(1).T-Blocks(“C1”).TReb);`

12 `Blocks(“C1”).QReb=TC42.OP-Blocks(“C2”).Condenser(1).Q;`

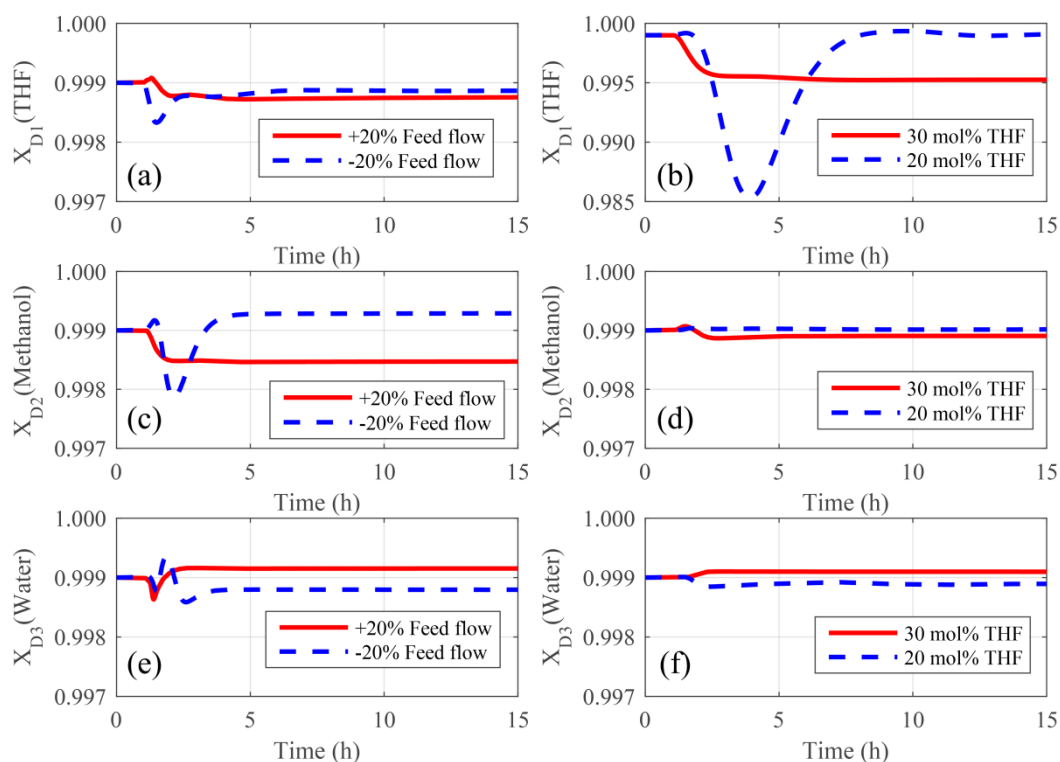
13 End

14 After the compiling the “flowsheet function”, the specification of  $QR1$  and  $QC2$  must be changed  
 15 to “free” state to ensure that the feasible dynamic runs. In addition, the output of the pressure  
 16 controller PC2 should be disconnected because of the heat integration [41].

17 Furthermore, the temperature controllers with detailed  $K_c$  and  $\tau_I$  in CS1 are summarized in  
 18 **Table S3**. Generally, the default maximum value for the transmitter range is set as the double times  
 19 of the initial value [39]. However, for the control of the partial heat-integrated distillation process in  
 20 this study, the maximum output of the TC2 controller is  $6.14 \text{ MW}$  which is much more than double  
 21 times of the steady state value (*i.e.*,  $0.15873 \text{ MW}$ ). The reason for increasing the maximum output is  
 22 to provide the enough supplements of reboiler duty and deal with the 20% disturbance. Meanwhile,  
 23 step changes in fresh feed flowrate and composition are introduced to test the anti-disturbance  
 24 capability. For instance, the fresh feed flowrate changes about  $\pm 20\%$  means that the flowrate varies  
 25 to 400 and 600 kmol/h, respectively. The 20% increase in the feed composition means that the new  
 26 feed conditions are set as: 30 mol% THF, 35 mol% methanol and 35 mol% water. Similarly, 20%  
 27 decrease composition disturbance implies that the new feed composition is as: 20 mol% THF, 40 mol%  
 28 methanol and 40 mol% water.

29 **Fig.4** presents the dynamic performances of the CS1 when  $\pm 20\%$  disturbances are introduced at 1

1 h and terminated at 15 h. Under the 20% disturbances of feed flowrate, it can be seen that the product  
 2 purities are all well maintained very close to the initial specifications (see **Fig.4 (a)-(c)-(e)**).  
 3 Moreover, CS1 can stabilize the system in the case of 20% feed composition disturbance. However,  
 4 the purity of THF cannot be efficiently controlled under the feed composition disturbance. As is  
 5 evident in **Fig.4 (b)**, the purity of THF performs a large transient deviation under the decreased  
 6 composition interference. And the stabilized value comes from 0.999 to 0.995 after introducing the  
 7 +20% composition disturbance which implies the great offset should be further reduced. Therefore,  
 8 the most important work in the following section is to find out a perfect control structure and  
 9 overcome the composition disturbance.

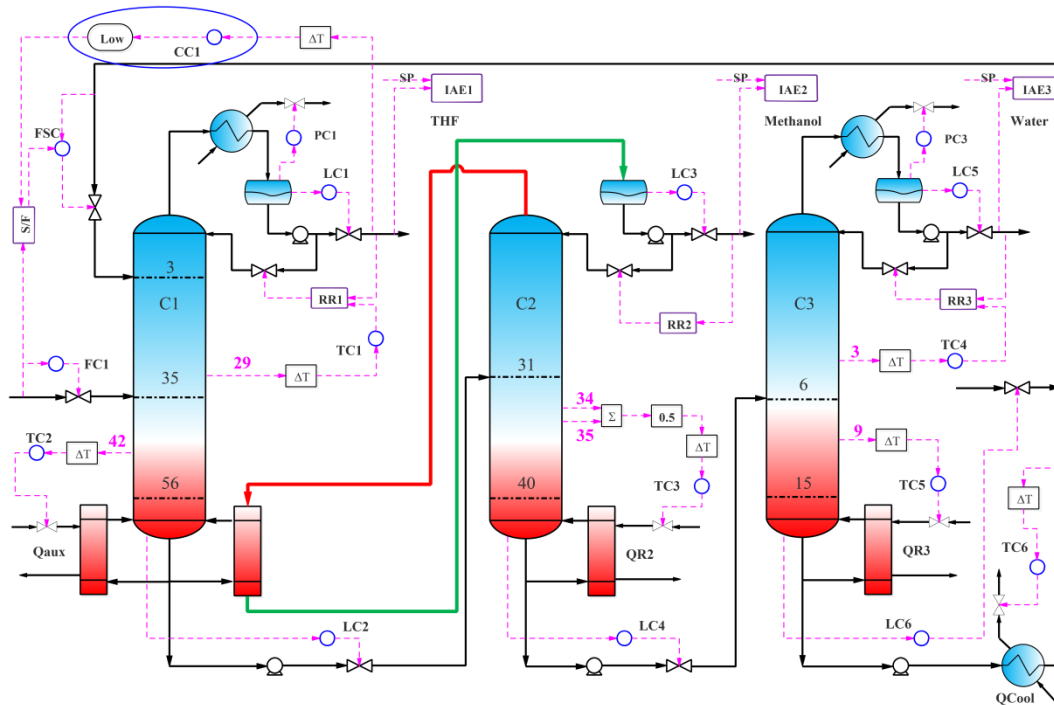


10  
 11 **Fig.4** The dynamic responses for the CS1 under the 20% disturbance of fresh feed flowrate and  
 12 composition

### 13 3.4 The control structure CS2 with composition-(S/F) cascade and a low selector

14 The CS1 cannot adjust the distilled stream in C1 column timely when the composition  
 15 disturbance is added. Especially, the purity of THF continuously decreases to 0.985 in a short time  
 16 under the increased 20% composition disturbance. One conjecture of this phenomenon is the CS1  
 17 lacks of a control loop for connecting the entrainer flowrate as well as the composition. In other  
 18 words, in order to break the azeotrope of THF-methanol and THF-water, the required DMSO of

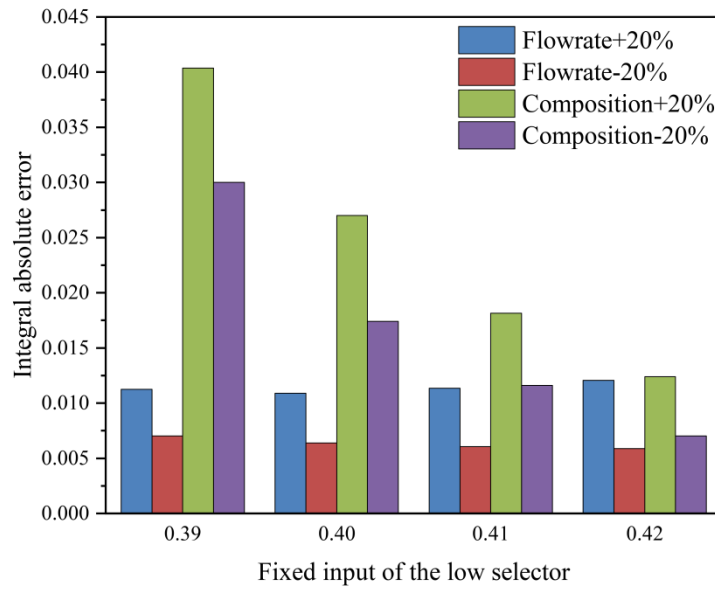
1 different amounts should be introduced when the feed composition is changed. Therefore, one  
 2 method to timely change the flowrate of DMSO is installing the composition controller. The  
 3 improved control structure CS2 is illustrated in **Fig.5**, Where the S/F value is applied to have a good  
 4 control of the purity of the THF component distilled from C1 column. When the purity of THF  
 5 comes to a higher value, the S/F ratio will reduce. Under the condition of optimal flowrate of the  
 6 recycled entrainer, the amount of DMSO is not expected to be highly declined. To achieve the  
 7 effective manipulation of S/F, the low selector is installed following the composition controller. The  
 8 controllability investigation study by using the selectors has been also presented by other works [8,  
 9 26, 35].



10  
 11 **Fig.5** The control structure of CS2 with composition-(S/F) cascade and a low selector for the  
 12 HITPED process

13 The low selector can make a decision on whether the output from the composition controller is  
 14 suitable to be transferred to the dynamic system. Herein, the fixed input of the low selector is set as  
 15 0.410 which means the maximum S/F value in the control system is 0.410. **Fig.6** gives the  
 16 comparison of the IAE values for different fixed input under the disturbances of feed flowrate and  
 17 feed composition. There is an IAE with much lower value when the fixed input of the low selector is  
 18 set to 0.420. However, when the increased flowrate disturbance is introduced to the control system,  
 19 the LC2 controller is easy to be saturated (see **Fig.S1**). Thereby, the low selector with 0.410 is finally

1 selected.

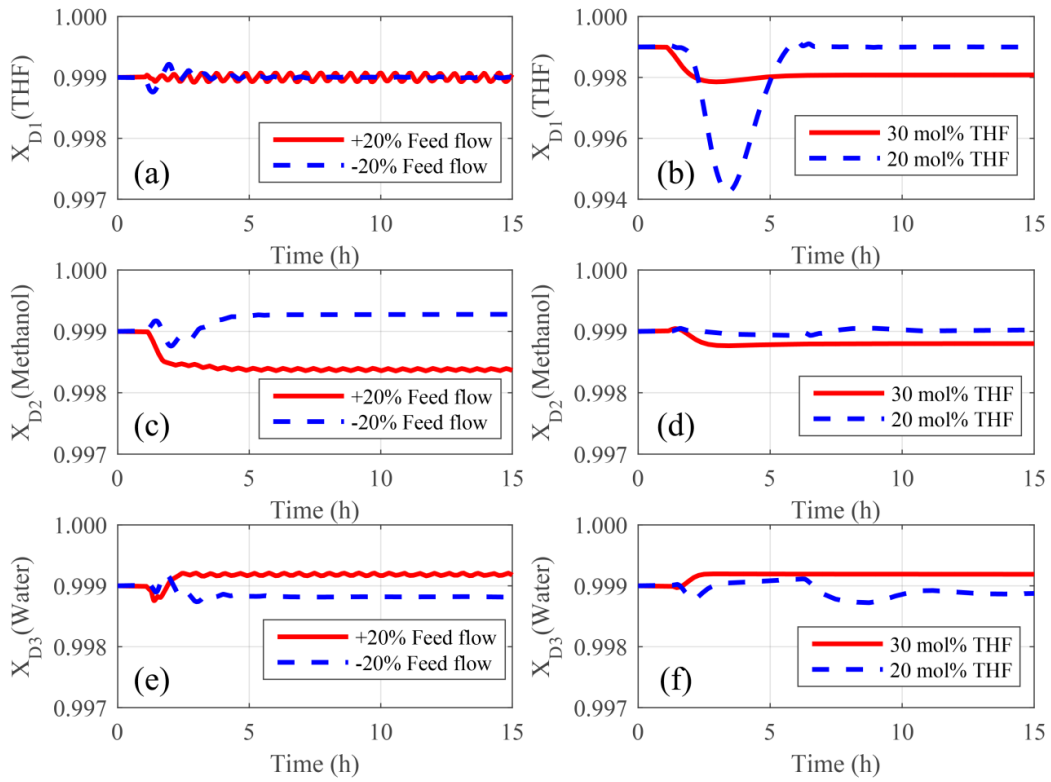


2

3 **Fig.6** The comparison of the integral absolute error (IAE) values under the different fixed input of  
4 the low selector

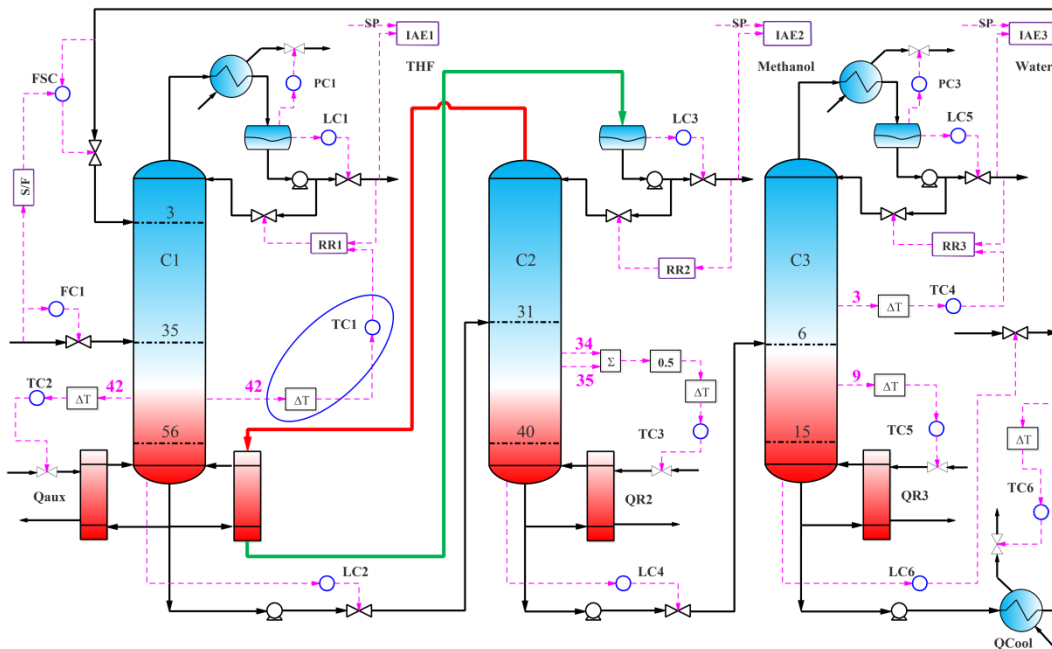
5 The tuning parameters of the temperature controllers and the composition controllers of C1  
6 column are all listed in the **Table S4**. The dynamic performances are shown in **Fig.7**. Very slight  
7 fluctuations occur under the increased disturbance of feed flowrate (**Fig.7 (a)-(c)-(e)**). When the feed  
8 flowrate comes to 600 kmol/h, the adjusted value of S/F is slightly fluctuating near the limit  
9 boundary leading to the accordingly oscillation in product purities. Above all, increasing the  
10 entrainer flowrate is beneficial to break the azeotrope of THF-methanol and THF-water. As is evident  
11 in **Fig.7 (b)** that the purity of THF can be well maintained near to the initial value after introducing  
12 the disturbance of 20% feed composition. The transient variation under the condition of decreased 20%  
13 composition has been reduced to 0.994, and the stabilized value when faced to increase 20%  
14 composition is 0.998. By comparison with anti-interference in CS1, the CS2 is more advanced.

15 However, the proposed CS2 is limited in practical processes since the composition controller has  
16 its drawback such as unreliability, high cost, and long delay [42]. As a result, whether the control  
17 structure without any composition controllers can be explored to efficiently handle the feed  
18 disturbances is the key objective in the following section.



1  
2 **Fig.7** The dynamic responses for the CS2 under the 20% disturbance of fresh feed flowrate and  
3 composition

4 3.5 The control structure CS3 with single temperature-sensitive tray for C1 column

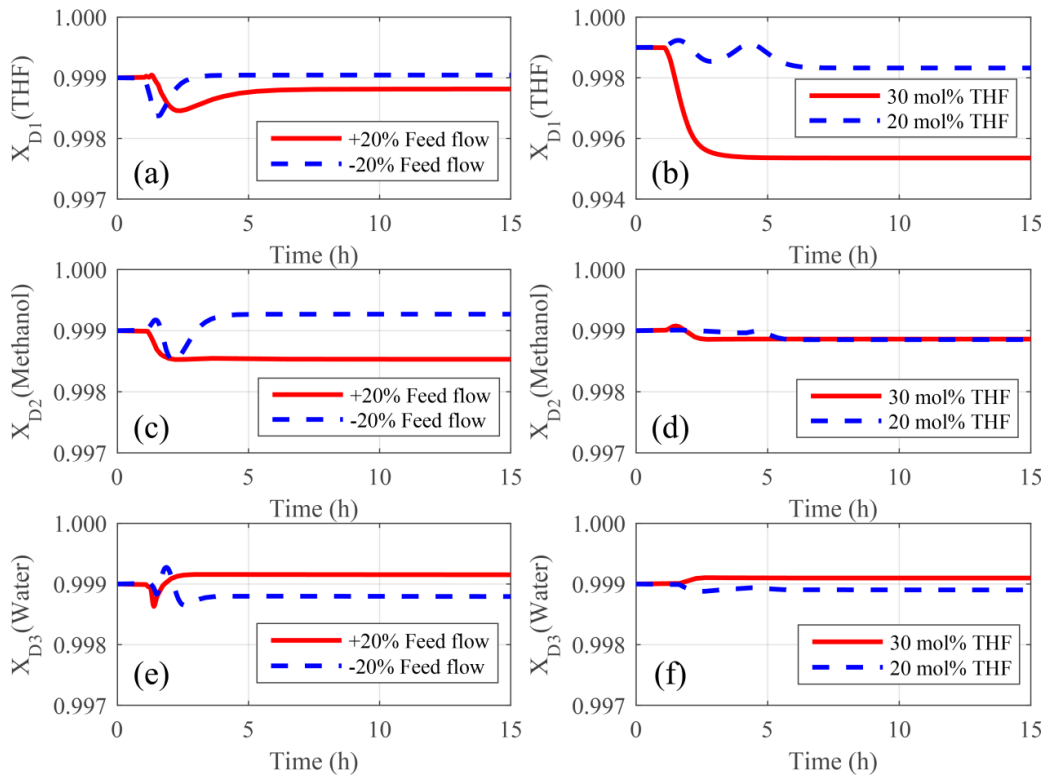


5  
6 **Fig.8** The control structure CS3 with single temperature-sensitive tray in C1 column for the HITPED  
7 process

8 In order to avoid using the costly composition controller, the temperature-sensitive plate is finally

1 changed, and only temperature controllers are considered. Different from the CS1, the temperature of  
 2 29th stage is not applied to control the RR1 in this section. It is proposed that the CS2 with  
 3 manipulating the RR1 and  $Q_{aux}$  to control the single temperature of 42th plate for C1 column, since  
 4 the largest temperature gain can be also obtained in the 42th tray in open-loop analysis under the  
 5 condition of the decreased RR1. And **Fig.8** provides the CS2 with detailed control schemes for the  
 6 HITPED process. Relay-feedback test is carried out again to obtain the suitable gains and integral  
 7 time along with the tuning parameters of temperature controllers are listed in **Table S5**.

8 The evaluation of the performance of the CS3 is carried out by introducing  $\pm 20\%$  feed flowrate  
 9 and composition disturbances at  $t=1$ h. **Fig.9 (a)-(c)-(e)** exhibits the dynamic responses under the feed  
 10 flowrate disturbance. It can be observed that CS3 always exhibits strong resistance to the  $\pm 20\%$   
 11 feed flowrate disturbance and the product purities are all controlled back close to the 99.9 mol% after  
 12 5 h. **Fig.9 (b)-(d)-(f)** demonstrates the dynamic results when faced to the  $\pm 20\%$  composition  
 13 disturbances. The purities of methanol and water are quickly stabilized and achieve the value near to  
 14 the 99.9 mol%. However, the red line in **Fig.9 (b)** demonstrates the offset for the purity of THF is  
 15 still high when faced to the increased feed composition disturbances, which should be further  
 16 improved.



17 **Fig.9** The dynamic responses for the CS3 under the 20% disturbance of fresh feed flowrate and  
 18

composition

### 3.6 The improved control structure CS4 with temperature-(S/F) cascade and a high selector

When the THF flowrate in feed increases (**Fig.9 (b)**), the flowrate of the entrainer is expected to be greater to achieve the high-purity product of THF. As such, a temperature control scheme is proposed with adjustable S/F value rather than the composition control structure CS2 with that. To select the appropriate stage of the specified temperature, the open-loop analysis for the change of the entrainer flowrate is then performed (**Fig.S2** in supporting information). Considering the hydraulic delay, the S/F value is manipulated by the temperature of the 21th stage in the C1 column. **Fig.10** demonstrates the improved control strategy with detailed signal connections.

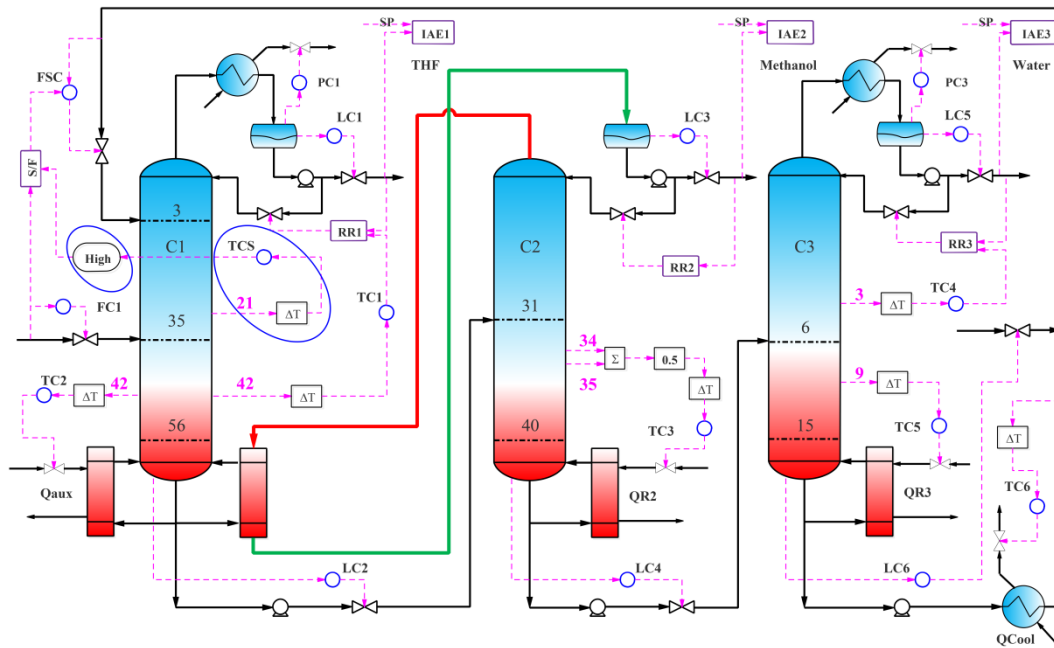
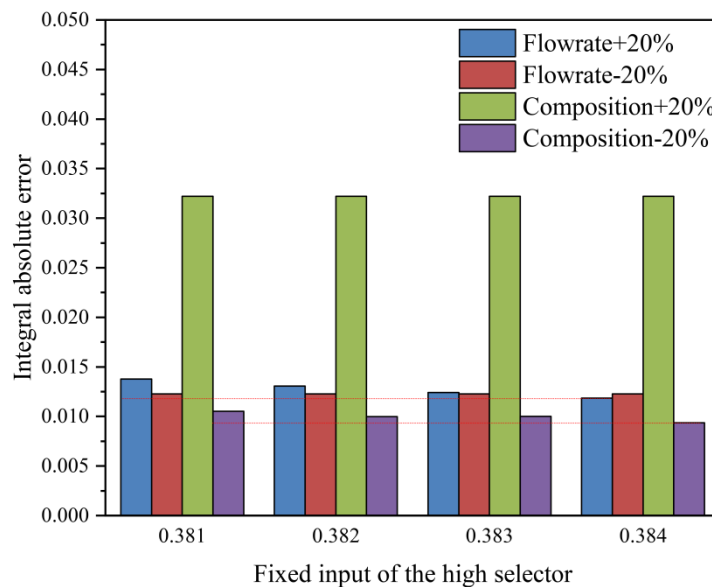


**Fig.10** The improved control structure with a high selector

It is noteworthy to mention that a high selector is added to maintain the entrainer flowrate cannot be smaller than the initial one. Moreover, the fixed input of the high selector is set as 0.384 (*i.e.*, the initial S/F value) which means the output value of the selector in the control system cannot be lower than 0.384. The determination of the significant value is illustrated in **Fig.11** which compared the IAE values for different input of the high selector under the feed disturbances. There are little difference under the disturbances of decreased feed flowrate and increased composition when choosing different values. However, the IAE value for the input of 0.384 is smaller under the

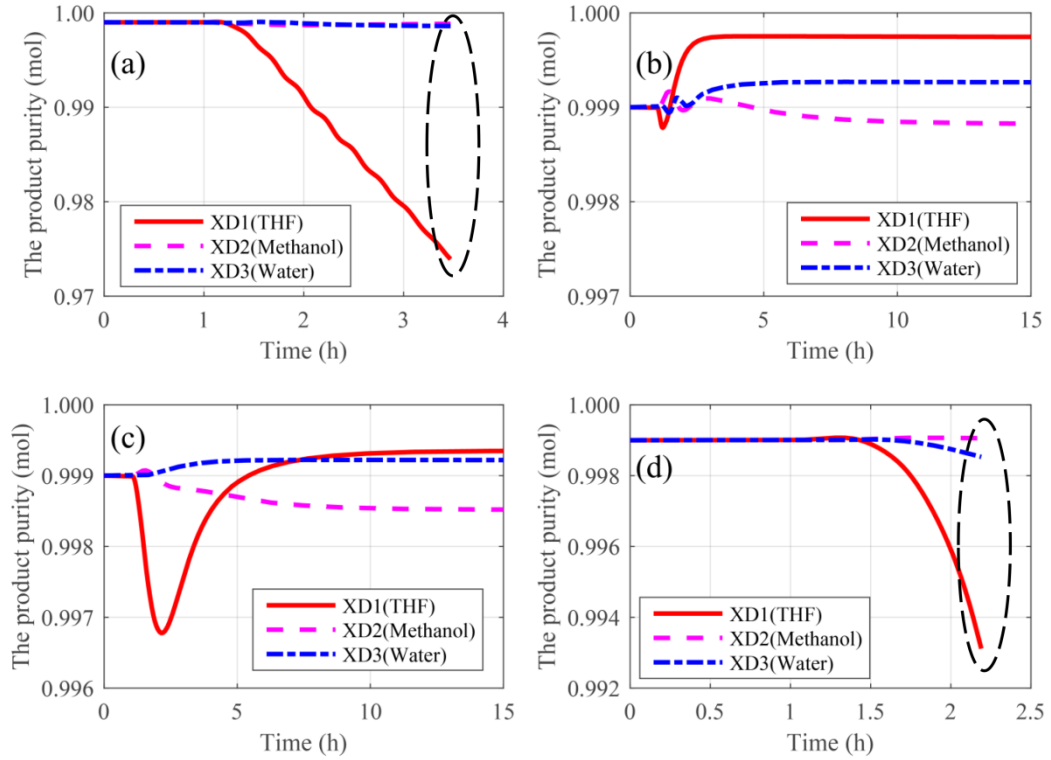
1 disturbances of increased feed flowrate and decreased composition. As a result, 0.384 is selected as  
 2 the final input of the high selector in CS4. In other words, no matter how the dynamic process  
 3 changes the flowrate of the entrainer is still enough to break the binary azeotrope in the C1 column.  
 4 To make the necessity clear of installing the high selector, the dynamic performance of the control  
 5 structure without the selector is given in **Fig.12**. There are some errors in the integral solver without  
 6 the assistance of a high selector when faced to the disturbances of the feed flowrate and composition.  
 7 And the corresponding dynamic simulation is shut down under the condition of the increased feed  
 8 flowrate and decreased composition (**Fig.12 (a)** and **(d)**). Especially, the purity of THF continuously  
 9 decreases with the flowrate of the recycled entrainer increasing dramatically. Therefore, the high  
 10 selector is necessary to ensure the dynamic process to be stable. Over again, the temperature  
 11 controllers with 1 min dead time are tuned by the Tyreus–Luyben method after the relay-feedback  
 12 tests. And the final setting parameters are summarized in the **Table S6**.



13

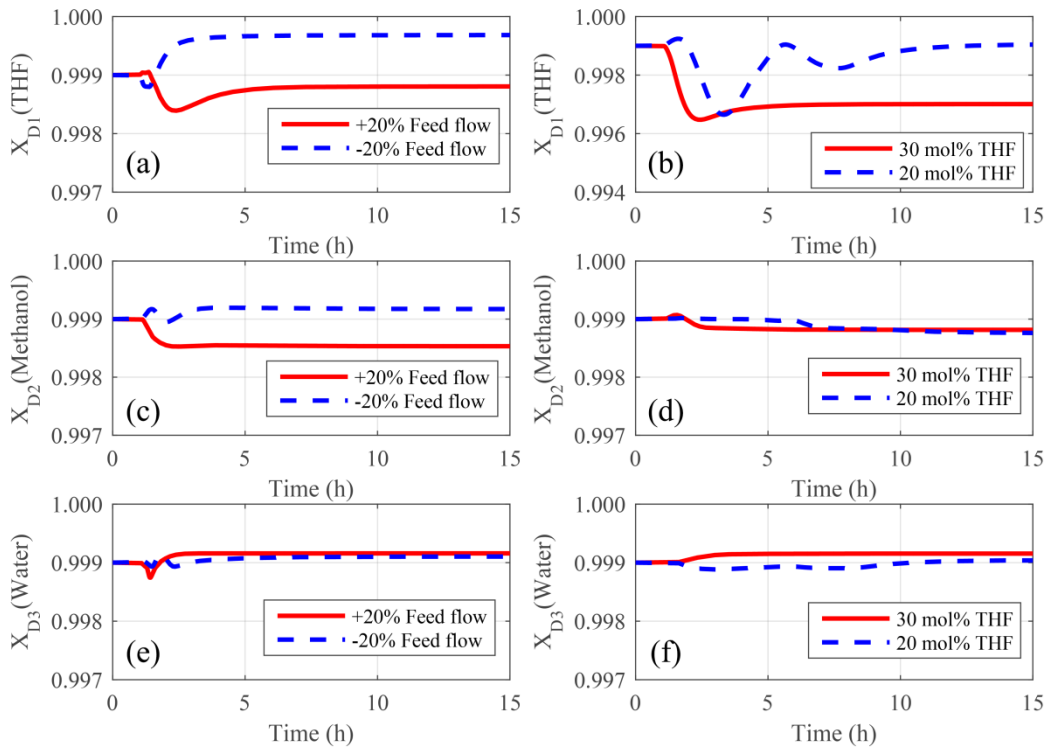
14 **Fig.11** The comparison of the integral absolute error (IAE) values under the different fixed input  
 15 of the high selector





1  
2  
3  
4

**Fig.12** The dynamic performances for the control structure without high selector under the disturbances of (a) +20% feed flowrate; (b) -20% feed flowrate; (c) +20% feed composition; (d) -20% feed composition



5  
6

**Fig.13** The dynamic responses for the CS4 under the 20% disturbance of fresh feed flowrate and

composition

The dynamic characteristic for the robust control strategy CS4 is indicated in **Fig.13**. The product purities could be quickly adjusted back to their desired values under the fresh feed flowrate disturbance. By comparison with the purity of methanol and water, it is found that the purity of THF has some greater deviation from the initial values after arriving at a new steady state under the decreased 20% feed flowrate interference (**Fig.13 (a)**). However, in this situation, the purity of THF comes to 0.9997 and it is also acceptable. **Fig.13 (b)** illustrates that the purity of THF has two damped oscillations under the decreased composition disturbance. And  $x_{D1}$  is eventually controlled back to a gratifying value close to 0.999. Comparatively, when increasing the fresh feed composition at 1 h, the purity of THF can be quickly returned back to a satisfactory steady-state value about 0.997. Moreover, both of the purities of methanol and water are well controlled under the 20% feed composition disturbances. Above all, dynamic performance of the robust control scheme CS4 is better than that of the previous CS3 for the complicated HITPED process. In this section, the CS4 is to improve the anti-interference ability for the THF purity under the feed composition disturbance.

#### 4 Comparison and discussion

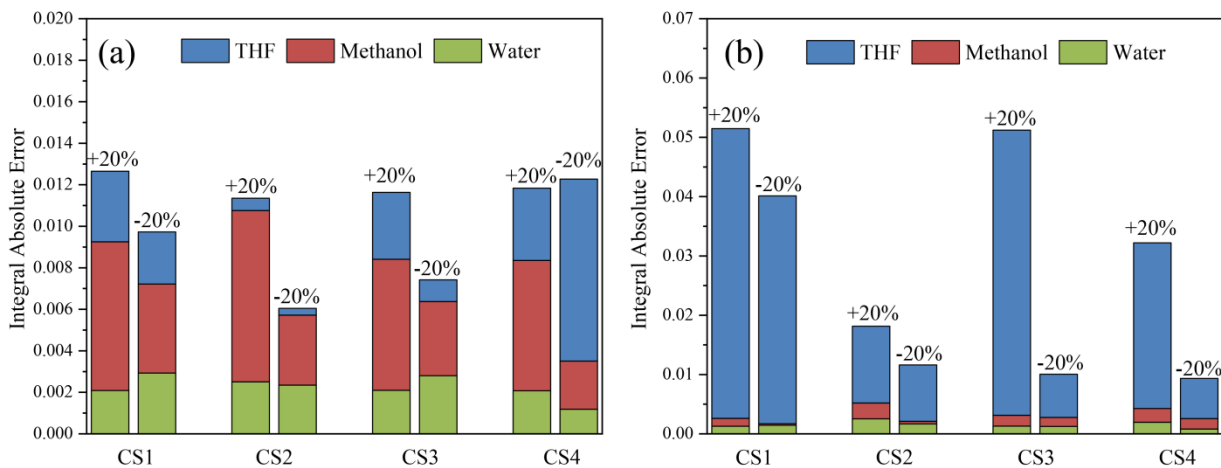


**Fig.14** The IAE comparison of the different control structures under the disturbances of (a)  $\pm 20\%$  feed flow rate disturbance; (b)  $\pm 20\%$  feed composition disturbance.

The IAE of products purities are calculated which are all obtained by installing IAE module (**Figs.3, 5, 8 and 10**). To clearly compare the dynamic performances of the three control schemes, the comparison of IAE for different control structures is displayed in **Fig.14**. All of the control structures can well deal with the feed flowrate disturbance while the dynamic performances are significantly

1 different under the composition perturbations. Meanwhile, the largest variation for the purity of THF  
2 exhibits a greater IAE value when the partial HITPED process faces to the feed composition  
3 interference (**Fig.14 (b)**). Both of the CS2 and CS4 exhibit dramatic improvements on dealing with  
4 the composition disturbances. By comparison of IAE, the CS2 has a better control effect of  
5 maintaining the product purities than that of CS4. Considering that the CS2 with composition  
6 controller is costly and long delayed in the industry process, the CS4 with temperature controllers  
7 has the superiority in the practical application. Above all, the CS4 is most effective in the practical  
8 application under the feed flowrate and composition disturbances.

## 9 5. Conclusions

10 Herein, the dynamic controllability of the heat-integrated triple-column pressure-swing extractive  
11 distillation (HITPED) was fully explored. Four different control schemes are displayed and the IAE  
12 was finally applied to compare the dynamic performance in terms of the product purities. The basic  
13 control structure with fixed the ratio of entrainer flowrate and feed flowrate (S/F value) was firstly  
14 obtained after determining the sensitive plates. However, the CS1 is not able to effectively deal with  
15 the composition disturbance because of the complexity of the partial HITPED process. To overcome  
16 the drawback of the large transient deviation of the THF purity under the composition disturbance in  
17 the CS1, an improved control structure CS2 with composition-(S/F) cascade and a low selector is  
18 investigated. By comparison, the CS2 performs better than the CS1 under the condition of changing  
19 the feed flowrate and composition. Nevertheless, the proposed CS2 has its defect owing to the long  
20 delay and large investments of composition controllers. Modified temperature control schemes (CS3  
21 and CS4) are then investigated to achieve the robust controllability. The CS4 with temperature-(S/F)  
22 cascade and a high selector can well deal with the 20% feed composition and flowrate disturbances.  
23 After the IAE comparison of different control structures, CS4 has shown the superiority in the  
24 industrial application and is suggested to be another valuable control scheme for the HITPED  
25 process.

26 It should be noted that the proposed control strategy can be further employed in the similar  
27 pressure-swing ED processes. The value of S/F is a key factor in the dynamic controllability for such  
28 processes. According to the different dynamic processes, the installation of the corresponding  
29 selector could be considered to maintain the adjustment in an appropriate range.

## 1 Author Information

2 Corresponding Author

3 E-mail: shenweifeng@cqu.edu.cn

## 4 Notes

5 The authors declare no competing financial interest.

## 6 Acknowledgments

7 We acknowledge the financial support provided by the National Natural Science Foundation of  
8 China (Nos. 21606026, 21878028); the Fundamental Research Funds for the Central Universities  
9 (No. 2019CDQYHG021).

## 10 Supporting information

11 The Supporting information is available free of charge *via* the Internet.

## 12 Nomenclature

13 THF Tetrahydrofuran

14 HITPED Heat-integrated triple-column pressure-swing extractive distillation process

15 RCMs Residue curve maps

16 PSD Pressure-swing distillation

17 ED Extractive distillation

18 DMSO Dimethyl sulfoxide

19 IAE Integral absolute error

20 S/F The ratio of the flowrate of recycled entrainer to the feed flowrate

## 21 References

22 [1] S. David, Lively, P. Ryan, Seven chemical separations to change the world, *Nature*, 532 (2016)  
23 435.

24 [2] Q. Zhang, M. Liu, A. Zeng, Performance enhancement of pressure-swing distillation process by  
25 the combined use of vapor recompression and thermal integration, *Comput. Chem. Eng.*, 120  
26 (2019) 30-45.

27 [3] W.L. Luyben, Comparison of Extractive Distillation and Pressure-Swing Distillation for  
28 Acetone–Methanol Separation, *Ind. Eng. Chem. Res.*, 47 (2008) 2696-2707.

29 [4] S. Liang, Y. Cao, X. Liu, X. Li, Y. Zhao, Y. Wang, Y. Wang, Insight into pressure-swing

- 1 distillation from azeotropic phenomenon to dynamic control, *Chem. Eng. Res. Des.*, 117 (2017)  
2 318-335.
- 3 [5] L. Hegely, P. Lang, Influence of entrainer recycle for batch heteroazeotropic distillation, *Front.*  
4 *Chem. Sci. Eng.*, 12 (2018) 643-659.
- 5 [6] I.L. Chien, K.L. Zeng, H.Y. Chao, J. Hong Liu, Design and control of acetic acid dehydration  
6 system via heterogeneous azeotropic distillation, *Chem. Eng. Sci.*, 59 (2004) 4547-4567.
- 7 [7] W. Shen, L. Dong, S.A. Wei, J. Li, H. Benyounes, X. You, V. Gerbaud, Systematic design of an  
8 extractive distillation for maximum-boiling azeotropes with heavy entrainers, *AIChE J.*, 61  
9 (2015) 3898-3910.
- 10 [8] T. Shi, A. Yang, S. Jin, W. Shen, S.A. Wei, J. Ren, Comparative optimal design and control of two  
11 alternative approaches for separating heterogeneous mixtures isopropyl alcohol-isopropyl  
12 acetate-water with four azeotropes, *Sep. Purif. Technol.*, 225 (2019) 1-17.
- 13 [9] E. Graczová, B. Šulgan, S. Barabas, P. Steltenpohl, Methyl acetate–methanol mixture separation  
14 by extractive distillation: Economic aspects, *Front. Chem. Sci. Eng.*, 12 (2018) 670-682.
- 15 [10] A.K. Jana, Heat integrated distillation operation, *Appl. Energy.*, 87 (2010) 1477-1494.
- 16 [11] Z. Zhu, L. Wang, Y. Ma, W. Wang, Y. Wang, Separating an azeotropic mixture of toluene and  
17 ethanol via heat integration pressure swing distillation, *Comput. Chem. Eng.*, 76 (2015)  
18 137-149.
- 19 [12] Q. Zhang, M. Liu, C. Li, A. Zeng, Heat-integrated pressure-swing distillation process for  
20 separating the minimum-boiling azeotrope ethyl-acetate and ethanol, *Sep. Purif. Technol.*, 189  
21 (2017) 310-334.
- 22 [13] A. Iqbal, S.A. Ahmad, Ojasvi, Design and control of an energy-efficient alternative process for  
23 separation of Dichloromethane-Methanol binary azeotropic mixture, *Sep. Purif. Technol.*, 219  
24 (2019) 137-149.
- 25 [14] Q. Zhang, M. Liu, W. Li, C. Li, A. Zeng, Heat-integrated triple-column pressure-swing  
26 distillation process with multi-recycle streams for the separation of ternary azeotropic mixture  
27 of acetonitrile/methanol/benzene, *Sep. Purif. Technol.*, 211 (2019) 40-53.
- 28 [15] A. Yang, W. Shen, S.A. Wei, L. Dong, J. Li, V. Gerbaud, Design and control of pressure-swing  
29 distillation for separating ternary systems with three binary minimum azeotropes, *AIChE J.*, 65  
30 (2019) 1281-1293.
- 31 [16] Y. Chen, C. Liu, Z. Geng, Design and control of fully heat-integrated pressure swing distillation  
32 with a side withdrawal for separating the methanol/methyl acetate/acetaldehyde ternary mixture,  
33 *Chem. Eng. Process. Proc. Intensification.*, 123 (2018) 233-248.
- 34 [17] C. Guang, X. Shi, Z. Zhang, C. Wang, C. Wang, J. Gao, Comparison of heterogeneous  
35 azeotropic and pressure-swing distillations for separating the  
36 diisopropylether/isopropanol/water mixtures, *Chem. Eng. Res. Des.*, 143 (2019) 249-260.
- 37 [18] Z. Zhu, D. Xu, H. Jia, Y. Zhao, Y. Wang, Heat Integration and Control of a Triple-Column

- 1 Pressure-Swing Distillation Process, *Ind. Eng. Chem. Res.*, 56 (2017) 2150-2167.
- 2 [19] S. Tututi-Avila, N. Medina-Herrera, J. Hahn, A. Jiménez-Gutiérrez, Design of an  
3 energy-efficient side-stream extractive distillation system, *Comput. Chem. Eng.*, 102 (2017)  
4 17-25.
- 5 [20] A. Yang, R. Wei, S. Sun, S.A. Wei, W. Shen, I.L. Chien, Energy-Saving Optimal Design and  
6 Effective Control of Heat Integration-Extractive Dividing Wall Column for Separating  
7 Heterogeneous Mixture Methanol/Toluene/Water with Multiazeotropes, *Ind. Eng. Chem. Res.*,  
8 57 (2018) 8036-8056.
- 9 [21] J. Gu, X. You, C. Tao, J. Li, Analysis of heat integration, intermediate reboiler and vapor  
10 recompression for the extractive distillation of ternary mixture with two binary azeotropes,  
11 *Chem. Eng. Process. Proc. Intensification.*, 142 (2019) 107546.
- 12 [22] X. You, J. Gu, C. Peng, W. Shen, H. Liu, Improved Design and Optimization for Separating  
13 Azeotropes with Heavy Component as Distillate through Energy-Saving Extractive Distillation  
14 by Varying Pressure, *Ind. Eng. Chem. Res.*, 56 (2017) 9156-9166.
- 15 [23] A. Yang, S. Sun, T. Shi, D. Xu, J. Ren, W. Shen, Energy-efficient extractive pressure-swing  
16 distillation for separating binary minimum azeotropic mixture dimethyl carbonate and ethanol,  
17 *Sep. Purif. Technol.*, (2019) 115817.
- 18 [24] A. Yang, H. Zou, I.L. Chien, D. Wang, S.A. Wei, J. Ren, W. Shen, Optimal Design and Effective  
19 Control of Triple-Column Extractive Distillation for Separating Ethyl Acetate/Ethanol/Water  
20 with Multiazeotrope, *Industrial & Engineering Chemistry Research*, 58 (2019) 7265-7283.
- 21 [25] Y. Li, C. Xu, Pressure-Swing Distillation for Separating Pressure-Insensitive Minimum Boiling  
22 Azeotrope Methanol/Toluene via Introducing a Light Entrainer: Design and Control, *Ind. Eng.*  
23 *Chem. Res.*, 56 (2017) 4017-4037.
- 24 [26] W.L. Luyben, Plantwide control of an isopropyl alcohol dehydration process, *AIChE J.*, 52  
25 (2006) 2290-2296.
- 26 [27] A. Yang, T. Shi, S. Sun, S.A. Wei, W. Shen, J. Ren, Dynamic controllability investigation of an  
27 energy-saving double side-stream ternary extractive distillation process, *Sep. Purif. Technol.*,  
28 225 (2019) 41-53.
- 29 [28] W.L. Luyben, Control of heat-integrated extractive distillation processes, *Comput. Chem. Eng.*,  
30 111 (2018) 267-277.
- 31 [29] Q. Pan, X. Shang, J. Li, S. Ma, L. Li, L. Sun, Energy-efficient separation process and control  
32 scheme for extractive distillation of ethanol-water using deep eutectic solvent, *Sep. Purif.*  
33 *Technol.*, 219 (2019) 113-126.
- 34 [30] S. Ma, X. Shang, M. Zhu, J. Li, L. Sun, Design, optimization and control of extractive  
35 distillation for the separation of isopropanol-water using ionic liquids, *Sep. Purif. Technol.*, 209  
36 (2019) 833-850.
- 37 [31] C. Wang, C. Wang, Y. Cui, C. Guang, Z. Zhang, Economics and Controllability of Conventional  
38 and Intensified Extractive Distillation Configurations for Acetonitrile/Methanol/Benzene

- 1 Mixtures, *Ind. Eng. Chem. Res.*, 57 (2018) 10551-10563.
- 2 [32] W.L. Luyben, Control of a Heat-Integrated Pressure-Swing Distillation Process for the  
3 Separation of a Maximum-Boiling Azeotrope, *Ind. Eng. Chem. Res.*, 53 (2014) 18042-18053.
- 4 [33] Y. Wang, Z. Zhang, H. Zhang, Q. Zhang, Control of Heat Integrated Pressure-Swing-Distillation  
5 Process for Separating Azeotropic Mixture of Tetrahydrofuran and Methanol, *Ind. Eng. Chem.  
6 Res.*, 54 (2015) 1646-1655.
- 7 [34] Z. Feng, W. Shen, G.P. Rangaiah, L. Dong, Proportional-Integral Control and Model Predictive  
8 Control of Extractive Dividing-Wall Column Based on Temperature Differences, *Ind. Eng.  
9 Chem. Res.*, 57 (2018) 10572-10590.
- 10 [35] Y. Li, Y. Jiang, C. Xu, Robust Control of Partially Heat-Integrated Pressure-Swing Distillation  
11 for Separating Binary Maximum-Boiling Azeotropes, *Ind. Eng. Chem. Res.*, 58 (2019)  
12 2296-2309.
- 13 [36] J. Gu, X. You, C. Tao, J. Li, V. Gerbaud, Energy-Saving Reduced-Pressure Extractive  
14 Distillation with Heat Integration for Separating the Biazeotropic Ternary Mixture  
15 Tetrahydrofuran–Methanol–Water, *Ind. Eng. Chem. Res.*, 57 (2018) 13498-13510.
- 16 [37] Z. Wang, Y. Su, W. Shen, S. Jin, J.H. Clark, J. Ren, X. Zhang, Predictive deep learning models  
17 for environmental properties: the direct calculation of octanol-water partition coefficients from  
18 molecular graphs, *Green Chem.*, 21 (2019) 4555-4565.
- 19 [38] Y. Su, Z. Wang, S. Jin, W. Shen, J. Ren, M.R. Eden, An Architecture of Deep Learning in QSPR  
20 Modeling for the Prediction of Critical Properties Using Molecular Signatures, *AIChE J.*, 65  
21 (2019) e16678.
- 22 [39] W.L. Luyben, Distillation Design and Control Using Aspen™ Simulation, *John Wiley & Sons*,  
23 2013.
- 24 [40] W.L. Luyben, I.L. Chien, Design and control of distillation systems for separating azeotropes,  
25 *John Wiley & Sons*, 2011.
- 26 [41] C.C. Yi, W. Shen, I.L. Chien, Design and control of an energy-efficient alternative process for  
27 the separation of methanol/toluene/water ternary azeotropic mixture, *Sep. Purif. Technol.*, 207  
28 (2018) 489-497.
- 29 [42] X. Qian, K. Huang, S. Jia, H. Chen, Y. Yuan, L. Zhang, S. Wang, Temperature difference control  
30 and pressure-compensated temperature difference control for four-product extended Petlyuk  
31 dividing-wall columns, *Chem. Eng. Res. Des.*, 146 (2019) 263-276.